Simple, fast and non-destructive method for detection of dimethylammonium impurity in photovoltaic methylammonium lead halides

M. Mączka, M. Ptak
Institute of Low Temperature and Structure Research, Polish Academy of Sciences, P.O.Box 1410, 50-950 Wrocław 2, Poland
E-mail: *m.maczka@int.pan.wroc.pl (M. Maczka)*

We show that Raman scattering can be used as simple, fast and non-destructive method for monitoring dimethylammonium (DMA^+) content in lead halide perovskites because this ion gives rise to a characteristic band at 888 cm^{-1}. In methylammonium lead bromide ($MAPbBr_3$) doped with DMA^+ cations, ratio of integrated intensities of the bands observed at 888 and 968 cm^{-1} is a linear function of DMA^+ content. We have also monitored growing of $MAPbBr_3$ from mixture containing N,N-dimethylformamide (DMF). This study shows that samples grown after 4, 20 and 72 h show 0, less than 1% and more than 10% of DMA^+. Our results show, therefore, that preparation of lead halides from solution containing DMF may lead to incorporation of DMA^+ cations and change of properties of the obtained materials. Our results also show that this problem as well as problem with degradation of metal halide perovskite precursor inks can be avoided using acetonitrile as a non-reactive and chemically stable solvent, instead of DMF. Use of acetonitrile and anti-solvent method with methyl acetate allows also growth of very large and good quality crystals within a few days.
Keywords: *lead halides, perovskite, photovoltaics, Raman, dimethylammonium*

1. Introduction

Lead halide perovskites of general formula $APbX_3$ (A= organic cation, X=Cl, Br, I) have received a lot of interest in recent years due to their photovoltaic and luminescent properties [1-3]. The most promising lead halides contain methylammonium (MA^+) cation [1,2]. These materials are usually processed for preparation of solar cells and thin-films using DMF as a solvent [1,2,4]. It has been realized quite recently that use of DMF may lead to incorporation of DMA^+ cations, created due to hydrolysis of DMF, in the $MAPbX_3$ structure [4]. This doping alter properties of the obtained materials. In particular, it was shown that doping of $MAPbI_3$ with DMA^+ stabilizes the cubic phase leading to better stability and performance of photodiodes [5]. Furthermore, it leads to strong enhancement in stability against moisture [5]. However, use of DMF leads also to serious problems in stability of metal halide perovskite precursor inks [6].

Herein, we report Raman study of representative example of lead halides, $MAPbBr_3$, pure and doped with DMA^+ cations, prepared using acetonitrile as the main solvent. For comparison sake, we also show Raman data for $MAPbBr_3$ prepared with use of DMF solvent. We will show that Raman spectroscopy is a very easy and fast method for monitoring content of DMA^+ impurity in the grown crystals.

2. Experiment

Single crystals of pure and DMA^+-doped $MAPbBr_3$ crystals were grown using antisolvent vapor-assisted crystallization, in which the appropriate antisolvent is slowly diffused into a solution containing the crystal precursors. In the typical synthesis, 4 mmol of hydrobromic acid was added to appropriate amounts of methanol solutions containing methylamine and dimethylamine (4 mmol). This mixture was then added to solution containing 2 mmol of $PbBr_2$, 3 mL of dimethyl sulfoxide (DMSO) and 5 mL of acetonitrile. The mixture was stirred, the obtained clear solution was transferred into a glass vial and this vial was placed in a second larger glass vial containing methyl acetate. The lid of the outer vial was thoroughly sealed but the lid of the inner vial was loosened to allow diffusion of the methyl acetate into the precursor solution. Orange crystals up to 20 mm were harvested after 3-5 days, washed with acetonitrile and dried at room temperature.

DOI : 10.18572/2619-0141-2018-2-3-2-16

In order to study the effect of time on possible contamination with DMA^+, we also performed synthesis of $MAPbBr_3$ using DMF/DMSO solvent. In this case, we have mixed 2 mmol of $PbBr_2$ with 4 mmol of methylammonium bromide, 5 mL of DMF and 2 mL of DMSO. The solution was kept in closed glass vials for 4, 20 and 72h. Then 5 mL of methanol was added and the resulting orange precipitate was washed 3 times with acetonitrile and dried.

For measurements of the absorption spectra, the Varian Cary 5E UV–vis-NIR spectrophotometer was used.

Raman spectra of the synthesized samples were measured in back-scattering configuration using Bruker FT 100/S spectrometer with the YAG:Nd laser excitation (1064 nm).

Table 1. Raman frequencies (in cm^{-1}) of $MAPbBr_3$ and $MAPbBr_3$: 60% DMA^+ together with suggested assignments.[a]

$MAPbBr_3$	$MAPbBr_3$: 60% DMA^+	assignment
3178w	3178w	ν (NH_3)
3116w	3108w	ν (NH_3)
	3043m	ν_{as} (CH_3)
3035w	3033m	ν_{as} (CH_3)
2966s	2965s	ν_s (CH_3)
	2908w	overtone?
2892w	2892w	ν (NH_3)
	2859w	ν_1 (HCOO) ?
2826w	2826w	ν (NH_3)
	2812w	$2\delta_{as}$ (CH_3)
1589m	1577m	δ_{as} (NH_3)
1477m	1475m	δ_s (NH_3)
	1456s	δ_s (CH_3)
	1437sh	ω(NH_2)
1425w	1426sh	δ_{as} (CH_3)
	1413w	τ(NH^2)
	1388w	ν_5 (HCOO) ?
	1348m	ρ (CH_3)
1249w	1249w	δ_s (C-N)
	1233w	ρ (CH_3)
	1073w	ρ (CH_3)
	1013w	ν_{as} (CNC)
968s	968s	ν_s (C-N)
918w	914w	ρ (NH_3)
	888s	ν_s (CNC)
	818w	ν_3 (HCOO) ?
	413w	δ (CNC)
321m	307m	C-N torsion

aKey: s, strong; m, medium; w, weak; sh, shoulder; ν, δ, ρ, ω and τ denote stretching, bending, rocking, wagging and twisting vibrations, respectively.

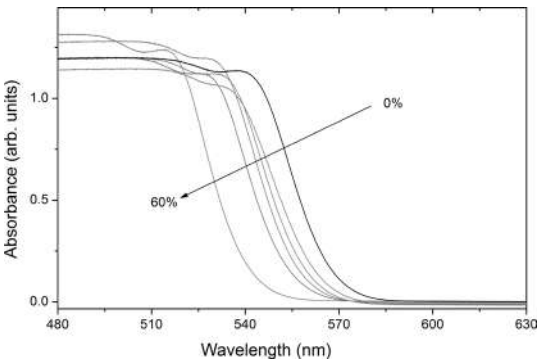

Fig. 1. The absorption spectra of pure $MAPbBr_3$ and $MAPbBr_3$ samples containing 5, 10, 15, 20 and 60 % of DMA^+.

3. Results and Discussion

Fig. 1 show room-temperature absorption spectra of the obtained samples. As can be seen, the absorption edge shifts to lower wavenumbers on DMA^+ doping and this shift is about 25 nm when going from $MAPbBr_3$ to $MAPbBr_3$: 60% DMA^+ sample. This behavior can be attributed to larger ionic size of DMA^+ compared to MA^+. Shift to lower wavenumbers indicates increase of the band gap what is disadvantageous for application in solar cells.

Raman spectra of the samples grown from acetonitrile/DMSO solution are presented in Figs. 2 and 3. Table 1 lists Raman bands observed for $MAPbBr_3$ and $MAPbBr_3$: 60% DMA^+ sample together with the proposed assignment. $MAPbBr_3$ shows presence of Raman bands at 1589 and 1477 cm-1 that can be attributed to NH_3 asymmetric

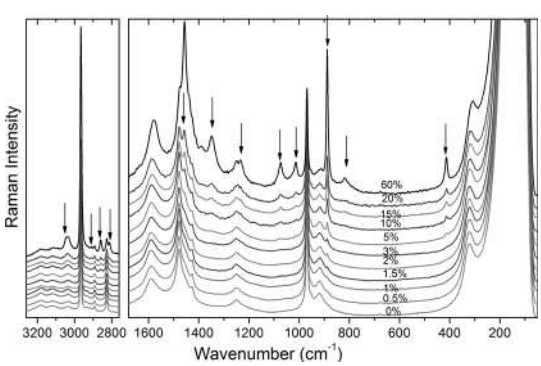

Fig. 2. Raman spectra of pure and DMA^+-doped $MAPbBr_3$ crystals grown from acetonitrile/DMSO solution. Arrows indicate bands that appear due to DMA^+ doping.

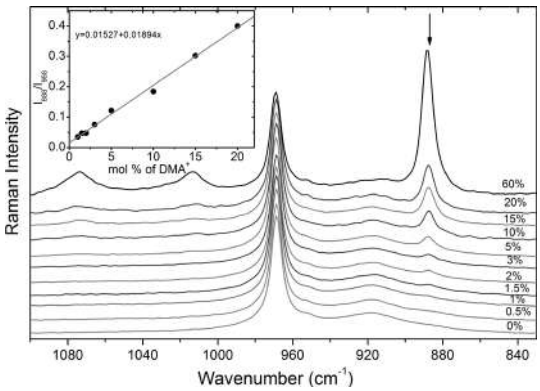

Fig. 3. Details of the Raman spectra of pure and DMA^+-doped $MAPbBr_3$ crystals grown from acetonitrile/DMSO solution. Inset shows ratio of integrated intensities of the bands observed at 888 and 968 cm^{-1} as a function of DMA^+ content.

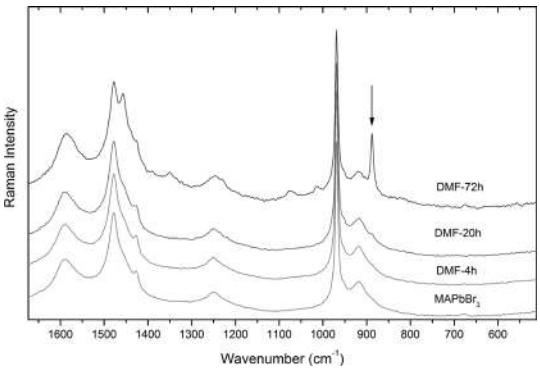

Fig. 4. Raman spectrum of $MAPbBr_3$ crystallized from acetonitrile/DMSO solution and $MAPbBr_3$ samples crystallized from DMF/DMSO solutions after 4, 20 and 72h.

and symmetric stretching modes, respectively [7,8]. Bands at 1456 and 1425 cm-1 are related to symmetric and asymmetric bending modes of the CH_3 groups, respectively whereas bands at 1249, 968, 918 and 321 cm-1 can be attributed to C-N symmetric bending, C-N symmetric stretching, NH_3 rocking and C-N torsion modes, respectively [7,8]. Doping with DMA^+ cations leads to appearance of a number of bands at 3043, 1456, 1437, 1413, 1348+1233+1073, 1013, 888 and 413 cm^{-1} that can be attributed to CH_3 asymmetric stretching, CH_3 bending, NH_2 wagging, NH_2 twisting, CH_3 rocking, C-N-C asymmetric stretching, C-N-C symmetric stretching and C-N-C bending modes, respectively [9,10]. There are also weak bands at 2908, 2859, 1388 and 818 cm-1. Origin of these bands is not clear but it is worth noting that similar bands were observed for formate frameworks [9-11]. We cannot, therefore, exclude that these weak bands appear due to presence of HCOO- ions that are formed during hydrolysis of DMF.

The most intense, narrow and well separated band of DMA^+ is that at 888 cm^{-1}. This band can be already visible for 1% of DMA^+ doping (see Fig. 3). Inset in Fig. 3 shows that ratio of integrated intensities of the bands observed at 888 and 968 cm^{-1} is a linear function of DMA^+ content, i.e., y=0.01527+0.01894x, where y=I888/I968 and x is mol % of DMA^+. Thus DMA^+ content in $MAPbBr_3$ can be estimated using this linear function. We expect that similar linear behavior should also be found for related $MAPbCl_3$ and $MAPbI_3$ compounds containing DMA^+ impurity.

Fig. 4 shows Raman spectra of $MAPbBr_3$ prepared from DMF/DMSO solution. As can be seen, when crystallization is performed after 4h, band at 888 cm^{-1} cannot be seen. Very weak band at 888 cm^{-1} appears, however, when synthesis is performed after 20h and when this time increase to 72h, this band becomes intense. We can estimate that the concentration of DMA^+ for this sample exceeds 10%. This result shows that it is very important to avoid longer synthesis time using DMF/DMSO mixture because such procedure may lead to large admixture of DMA^+ impurity. Methylammonium lead halide precursor inks containing DMF should not be stored for a longer time due to degradation of such inks leading to appearance of DMA^+ impurity. The best results can be obtained when using acetonitrile/DMSO mixture since in this case growth for a prolonged time or keeping of precursor inks will not alter stoichiometry of the obtained perovskite thin films, crystals, solar cells etc.

4. Conclusions

We show that $MAPbBr_3$ can be easily doped with DMA^+ ions and that ratio of integrated intensities of the bands observed at 888 and 968 cm-1 can be used for monitoring DMA^+ content in the samples. This method is very fast, easy and non-destructive thus it is very suitable for monitoring chemical composition of solar cells and thin films prepared from lead halide perovskites that lead to modification of the band gap, structure and properties of these devices. It should also be suitable for monitoring DMA^+ impurity in metal halide perovskite precursor inks.

DOI : 10.18572/2619-0141-2018-2-3-2-16

References

[1] Y. Chen, M. He, J. Peng, Y. Sun, Z. Liang, Structure and Growth Control of Organic–Inorganic Halide Perovskites for Optoelectronics: From Polycrystalline Films to Single Crystals, Advanced Science. 3 (2016) 1500392.

[2] Z. Shi, A.H. Jayatissa, Perovskites-based solar cells: a review of recent progress, materials and processing methods, Materials. 11(5) (2018) 729.

[3] X. Zhao, J.D.A. Ng, R. H. Friend, Z.K. Tan, Opportunities and Challenges in Perovskite Light-Emitting Devices, ACS Photonics. 5(10) (2018) 3866-3875.

[4] M.V. Lee, S.R. Raga, Y. Kato, M.R. Leyden, L.K. Ono, S. Wang, Y. Qi, Transamidation of dimethylformamide during alkylammonium triiodide film formation for perovskite solar cells, Journal of Materials Research. 32(1) (2017) 45-55.

[5] Z. Shi, Y. Zhang, C. Cui, B. Li, W. Zhou, Z. Ning, Q. Mi, Symmetrization of the crystal lattice of MaPbI3 boosts the performance and stability of metal-perovskite photodiodes. Advanced Materials. 29(30) (2017) 1701656.

[6] B. Dou, L.M. Wheeler, J. A. Christians, D.T. Moore, S.P. Harvey, J.J. Berry, F.S. Barnes, S.E. Shaheen, M.F.A.M. van Hest, Degradation of highly alloyed metal halide perovskite precursor inks: mechanism and storage solutions, ACS Energy Letters. 3(4) (2018) 979-985.

[7] A.M.A. Leguy, A.R. Goni, J.M. Frost, J. Skelton, F. Brivio, X. Rodriguez-Martinez, O.J. Weber, A. Paltipurath, M.I. Alonso, M. Campoy-Quiles, M.T. Weller, J. Nelson, A. Walsh, P.R.F. Barnes, Dynamic disorder, phonon lifetimes, and the assignment of modes to the vibrational spectra of methylammonium lead halide perovskites, Physical Chemistry Chemical Physics. 18(39) (2016) 27051-27066.

[8] M. Ptak, M. Mączka, A. Gagor, A, Sieradzki, A. Stroppa, D. Di Sante, J.M. Perze-Mato, L. Macalik, Experimental and theoretical studies of structural phase transition in a novel perovskite-like [C2H5NH3][Na0.5Fe0.5(HCOO)3] formate, Dalton Transactions. 45(6) (2016) 2574-2583.

[9] M. Mączka, M. Ptak, L. Macalik, Infrared and Raman studies of phase transitions in metal-organic frameworks of [(CH3)2NH2][M(HCOO)3] with M=Zn, Fe, Vibrational Spectroscopy. 71 (2014) 98-104.

[10] M. Mączka, W. Zierkiewicz, D. Michalska, J. Hanuza, Vibrational properties and DFT calculations of the perovskite metal formate framework of [(CH3)2NH2][Ni(HCOO)3] system, Spectrochimica Acta - Part A: Molecular and Biomolecular Spectroscopy. 128 (2014) 674-680.

[11] M. Mączka, A. Gagor, M. Ptak, W. Paraguassu, T. Almeida da Silva, A. Sieradzki, A. Pikul, Phase transitions and coexistence of magnetic and electric orders in the methylhydrazinium metal formate frameworks, Chemistry of Materials. 29(5) (2017) 2264-2275.